













IDENTIFICATION OF POTENTIAL CO₂ INJECTION ZONES IN THE SERRA GERAL GROUP: A GEOPHYSICAL ANALYSIS OF LEGACY DRILLED WELLS

Antônio Rosales Gonçalves Oliveira¹ ; João Pedro Tauscheck Zielinski¹ ; Erico Albuquerque Dos Santos¹ ; Stéphanie Carvalho da Silva¹ ; William Jeovanini Fucks¹ ; Pedro Costabile de Souza² ; Rodrigo Sebastian Iglesias¹ ; Breno Leitão Waichel³ ; Victor Hugo Jacks M dos Santos¹ ; Felipe Dalla Vecchia¹ ; Cassiane Maria Nunes Ferreira⁴ ; Leonildes Soares de Melo Filho⁴ 

1 – Instituto do Petróleo e dos Recursos Naturais - PUCRS. Av. Ipiranga, 6681 - Prédio 96J - Partenon, Porto Alegre - RS, 90619-900. E-mail: antonio.oliveira9@hotmail.com; joao.zielinski@pucrs.br; erico.santos@pucrs.br; stephanie.silva@pucrs.br; william.fucks@pucrs.br; rodrigo.iglesias@pucrs.br; victor.santos@pucrs.br; felipe.vecchia@pucrs.br

2 - Departamento de Geologia. Universidade Federal do Rio Grande do Sul (UFRGS). Av. Bento Gonçalves, 9500 - Agronomia, Porto Alegre - RS, 91509-900. E-mail: pedro.costabile@gmail.com

3 - Departamento de Geologia. Universidade Federal de Santa Catarina (UFSC). Campus Reitor João David Ferreira Lima – Trindade, Florianópolis – SC – Brasil, 88040-900 E-mail: breno@cfh.ufsc.br

4 – REPSOL SINOPEC. Av. Ipiranga, 6681 – Porto Alegre, RS, 90619-900. E-mail: cassiane.ferreira@repsolsinopec.com; leonildes.soares@repsolsinopec.com

Abstract: *The Serra Geral Group (SGG) in the Paraná Basin have gained attention due to their potential for CO₂ mineralization. Despite its vast extent (~787,000 km²), geological data are limited, hindering the identification of suitable storage zones. This study proposes an integrated workflow based on geophysical log interpretation from four wells (1-PT-1-PR, 2-AN-1-PR, 1-API-1-PR and 1-AV-1-PR) located in a region with potential for CO₂ geological storage. Well 1-PT-1-PR was used as a reference model due to its comprehensive geophysical dataset and the revealed intercalation patterns of flow interiors and interflow horizons. Porosity was estimated using a velocity-porosity relationship based on P-wave velocities. High-porosity zones ($\Phi > 10\%$) were identified, associated with flow tops or bases, and compound flows. High-porosity zones exhibited low density (~2 g/cm³), porosity values up to 30%, and low P-wave velocities (~3.1 km/s). Additional high-porosity intervals were identified in the other wells, with “net-to-gross” ratios ranging from 19% to 43%. Gamma ray peaks, positive caliper log excursions, and reduced resistivity values supported the presence of altered and porous zones. The recurrence of high-porosity intervals and their potential lateral continuity indicate the feasibility of future CO₂ injection. The workflow applied in this study enhances the understanding of lava flow architecture in the SGG and provides a framework for identifying prospective CO₂ injection zones. Future work will focus on sub-regional correlation to support site-specific mineralization projects.*

Keywords – CCUS; volcanic reservoir; borehole geophysics; Paraná Basin; Brazil.

1. INTRODUCTION

The injection of anthropogenic CO₂ into deep geological formations is considered a promising strategy for climate change mitigation, primarily due to the wide availability and global distribution of suitable subsurface reservoirs (Shaw & Bachu, 2002; Oelkers & Cole, 2008; Gislason et al., 2011). This approach, known as Carbon Capture and Storage (CCS), comprises injecting CO₂ into porous rock formations, typically at depths greater than 800 meters, where pressure and temperature conditions favor long-term containment and geochemical stability. Among the various types of geological formations considered viable for CO₂ storage - including saline aquifers, depleted hydrocarbon reservoirs, and unmineable coal seams - basaltic formations have recently gained attention as viable CO₂ storage sites due to their ability to rapidly mineralize CO₂ into stable carbonates, offering a secure long-term solution (Oelkers et al., 2008).

Volcanic rocks of the Serra Geral Group (SGG) in the Paraná Basin have been the focus of numerous studies in recent years due to their

potential for CO₂ mineralization (Zielinski et al., 2024a; Zielinski et al., 2024b). The SGG spans in portions of Brazil's South, Southeast, and Midwest regions, covering with an estimated area of 787,000 km² (calculated from SGB, 2022). However, geological data from these volcanic rocks are publicly available for only 82 exploratory drilling wells (ANP, 2020).

Furthermore, the heterogeneities of these volcanic rocks present challenges in accurately identifying potential horizons (reservoir intervals and seals) for optimal CO₂ injection. This study aims to propose a workflow for delineating lava flows and identifying potential intervals for CO₂ injection, leveraging the limited available data through geophysical analysis.

2. MATERIALS AND METHODS

To enhance the understanding of the lava flows occurrences and their petrophysical properties, data from four exploratory wells (1-PT-1-PR, 2-AN-1-PR, 1-API-1-PR and 1-AV-1-PR) located in a recently identified area potentially suitable for CO₂ geological storage (Zielinski et al., 2024a) were analyzed (Fig. 1).

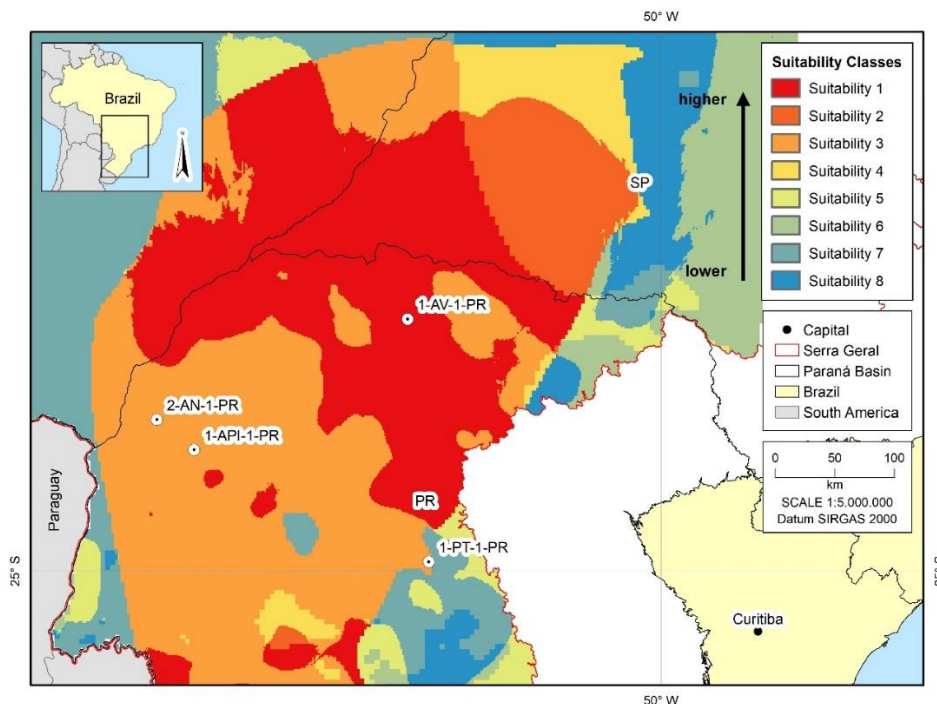


Figure 1. Suitability classes of the Serra Geral Group for CO₂ storage based on multicriteria geological analysis, highlighting the locations of wells analysed in this study within Paraná State. Source: Adapted from Zielinski et al. (2024a).

The well 1-PT-1-PR was selected as a reference model due to its comprehensive geophysical dataset for the basalt interval, which includes sonic slowness (DT), bulk density (RHOB), neutron porosity (NPHI), induced deep resistivity (ILD), gamma ray (GR), and caliper (CALI) logs (Table 1). To further enhance the analysis, the P-wave velocity (Vp) was derived from the sonic DT log data. Although the SGG rocks in the reference well do not extend to a depth of 1,000 meters - a potential target depth for CO₂ mineralization to mitigate the risk of contaminating drinking water aquifers - the well provides valuable insights into the occurrence and cyclicity of lava flows.

Table 1. Geophysical data used for each borehole.

Well	Depth analyzed	Geophysical log	Source
1-PT-1-PR	675 – 900 m	DT, RHOB, NPHI, ILD, GR and CALI	
2-AN-1-PR	900 – 1,200 m	DT, GR, ILD and CALI	ANP-REATE
1-AV-1-PR	900 – 1,200 m	DT, GR, ILD and CALI	(2020)
1-API-1-PR	900 – 1,200 m	DT, GR, ILD and CALI	

The Botucatu Formation lies stratigraphically beneath the SGG and constitutes a major aquifer capable of supplying significant amounts of potable water. Given its importance and active use by local populations, a 100-meter safety distance was implemented to mitigate potential contamination risks. The knowledge obtained by analyzing the reference well was applied to other three wells with optimal depth intervals between 900 to 1,200 m. This depth interval emerges as a prospective interval due to its estimated temperature and pressure to facilitate the CO₂ mineralization considering the basin's geothermal gradient. In well 1-PT-1-PR, the Botucatu Formation (part of the Guarani Aquifer)

is found at a depth of 985 m, with two intertrap sedimentary layers located between 912 – 914 meters and 952 – 964 m. To avoid potential conflicts or interference, the analyzed interval was limited to depths between 675 and 900 m. This selection ensures compliance with the minimum reference depth of 800 meters required for CCS technology, providing sufficient pressure and temperature for mineralization and minimizing leakage risks of contamination in the Guarani Aquifer.

Wireline log interpretation in flood basalt provinces has been discussed in detail in works such as Planke (1994), Helm-Clark et al. (2004), Andersen et al. (2009) and Nelson et al. (2009; 2015), which provided the interpretive frameworks applied in this study. Planke (1994) demonstrated in his study from the Vøring Margin that the internal architecture of basaltic lava flows can be interpreted using wireline logs. A typical flood basalt flow comprises three distinct zones: i) a vesicular or fractured rubbly crust; ii) a massive core with high density and velocity; and iii) a thin vesicular base (Nelson et al., 2009; Nelson et al., 2015). While the core and crust are easily identified through density and sonic logs, weathered flow tops are marked by increased gamma ray values and low acoustic velocities. Due to their limited thickness, basal zones are often below the detection threshold of standard wireline log resolution. In general, resistivity is widely recognized as a key geophysical log for distinguishing between low-porosity flow interiors and high-porosity flow tops, due to its strong sensitivity to variations in porosity, pore fluid saturation, and clay content (Navarro et al., 2020). Typically, basalt flow interiors exhibit very high resistivity values - often exceeding 1,000 Ω•m - because of their low porosity and reduced amounts of conductive fluid. In contrast, flow boundaries and interbeds tend to show lower resistivity, attributed to increased porosity and compositional changes that favor fluid retention (Helm-Clark et al., 2004).

3. RESULTS AND DISCUSSIONS

In well 1-PT-1-PR, the 675 – 900 m interval encompasses four distinct lava flows, which were categorized into two types: (a) low-porosity units, represented by massive flow cores; and (b) high-porosity units ($\Phi > 10\%$ [Rossetti et al., 2019]), represented by vesicular or brecciated flow tops and bases and compound pahoehoe flows. For CO₂ geological storage, potential injection points should prioritize rocks with higher porosity (Rasool et al., 2023) (e.g., upper portions of brecciated or vesicular lava flows), while rocks with lower porosity (e.g., center portions of massive lava flows) are interpreted as potential seals.

In the selected interval of 1-PT-1-PR, higher porosity conditions were identified in four different horizons with thicknesses ranging from 13.4 to 17.4 m. The petrophysical properties showed sonic log values between 72 and 98.2 $\mu\text{s}/\text{ft}$, density log values of approximately 2 g/cm^3 , NPHI of 37.2 %, CALI measurements indicate up to 3.75 inches difference to the bit size, and p-wave velocities as low as 3.1 km/s. The ILD values in these zones range from 35 to 74 $\Omega \cdot \text{m}$, suggesting the presence of pore-filling fluids and/or clay minerals associated with weathering or alteration processes. These results are aligned with studies associating these characteristics with the presence of vesicles and/or fractures that classify this portion as high-porosity horizons (Helm-Clark et al., 2004; Navarro et al., 2020).

The Vp-porosity reached values of up to 30 %, slightly different than those measured with NPHI.

The difference observed arises from the fact that each method relies on distinct petrophysical response. The neutron porosity (NPHI) method estimates porosity by measuring the neutron count, which is related to the hydrogen content in the rock (Broglia & Ellis, 1990). Conversely, porosity derived from the sonic log (DT) is calculated based on the velocity at which acoustic waves propagate through the formation.

In contrast, lower porosities conditions were identified in flows with thicknesses ranging from 21 to 76 m, sonic values restricted between 50 and 54 $\mu\text{s}/\text{ft}$, density log values up to 2.96 g/cm^3 , NPHI as low as 5.05%, caliper diameter on the order of 13 inches (12¼-inch bit size), and p-wave velocities as high as 6.05 km/s, indicating the presence of flow interiors that suggest their potential as seals. The sonic-derived porosity reached values as low as 2.66 %, which is consistent with laboratory porosity values from rock plugs. These results demonstrate that these intervals have a higher density, higher p-wave velocities and, consequently, low porosity.

The behavior presented in the reference well (Figure 2) is characteristic of tabular flows as seen in Nelson et al. (2009), where the flow core presents restricted higher velocities, higher densities and lower porosity. Positive spikes in GR found at around 700, 775 and 825-m horizons can be correlated to weathered and altered conditions as the gamma ray (GR) log primarily responds to elevated potassium concentrations associated with alteration clays such as smectite and celadonite (Planke, 1994).

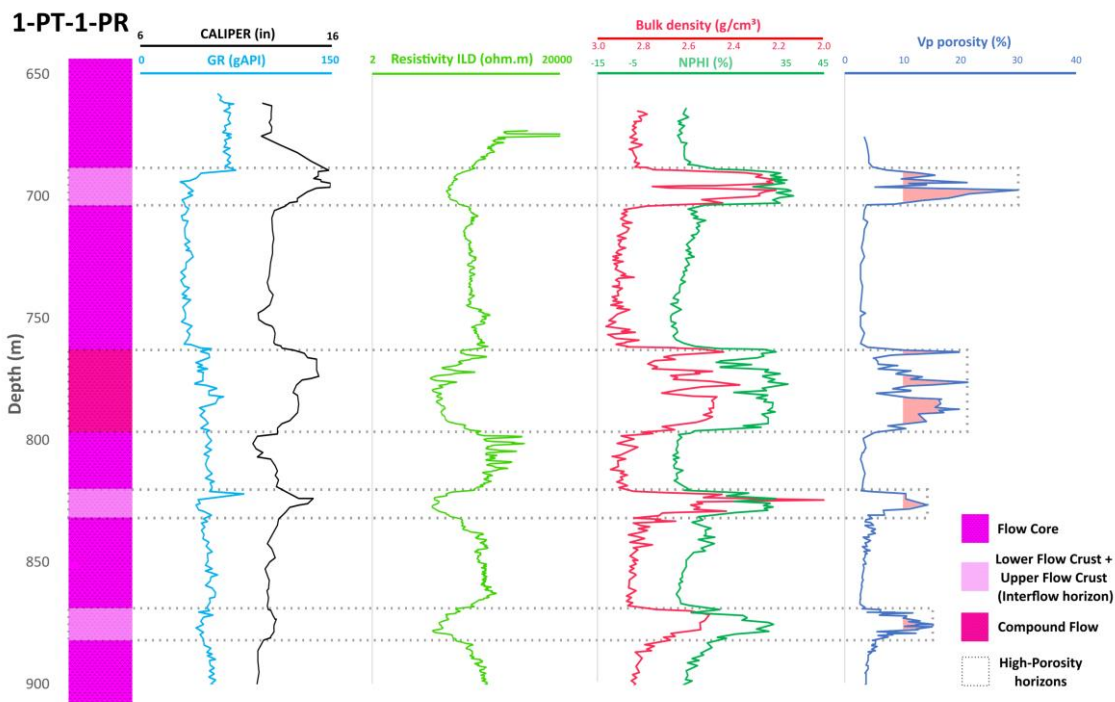


Figure 2. Reference well 1-PT-1-PR and the respective geophysical logs used in the interpretations. Source: elaborated by the authors with data from ANP (2020).

These conditions are commonly found in subaerially weathered interflow sediments and in fractured or vesicular flow tops (Planke, 1994). Nelson et al. (2015) described the same observations regarding the GR positive spikes in subaerial lava flows found in West Greenland. The classification into high- and low-porosity units is relatively straightforward; however, distinguishing between the upper and lower flow crusts depends on subtle variations in the wireline logs. Consequently, the categorization presented in this study into only three units—Flow Core, Interflow horizon, and Compound Flow—reflects a more conservative approach than that employed in the aforementioned studies. A clearer understanding of these intervals and their cyclicity in the reference well will aid in the effective planning of a future injection well and in defining the appropriate casing requirements.

In well 2-AN-1-PR, 11 high-porosity intervals were found, ranging from 0.9 to 30 m in thickness, with an average of 7 m and an average

porosity of ca. 18 %. Collectively, these intervals sum to about 130 m, resulting in a “net-to-gross” (proportion of a rock volume that is considered a potential reservoir-quality relative to the total rock volume) of 43%, with particular emphasis on the interval between 1,170 and 1,200 m (Figure 3a) where a 30-m horizon was identified. The temperature estimated from the geothermal gradient for the 900 – 1,200 m interval ranges from 40 to 46 °C.

In well 1-API-1-PR, 11 high-porosity intervals were also identified, averaging 21 % porosity. Thicknesses range from 0.7 to 11.2 m, with a mean of 3.5 m, totaling 56 m of high-porosity zones. This corresponds to “net-to-gross” of 19%. Notably, three of these intervals are concentrated between 1,050 and 1,090 m (Figure 3b). The temperature estimated from the geothermal gradient for the 900 – 1,200 m interval ranges from 42 to 49 °C.

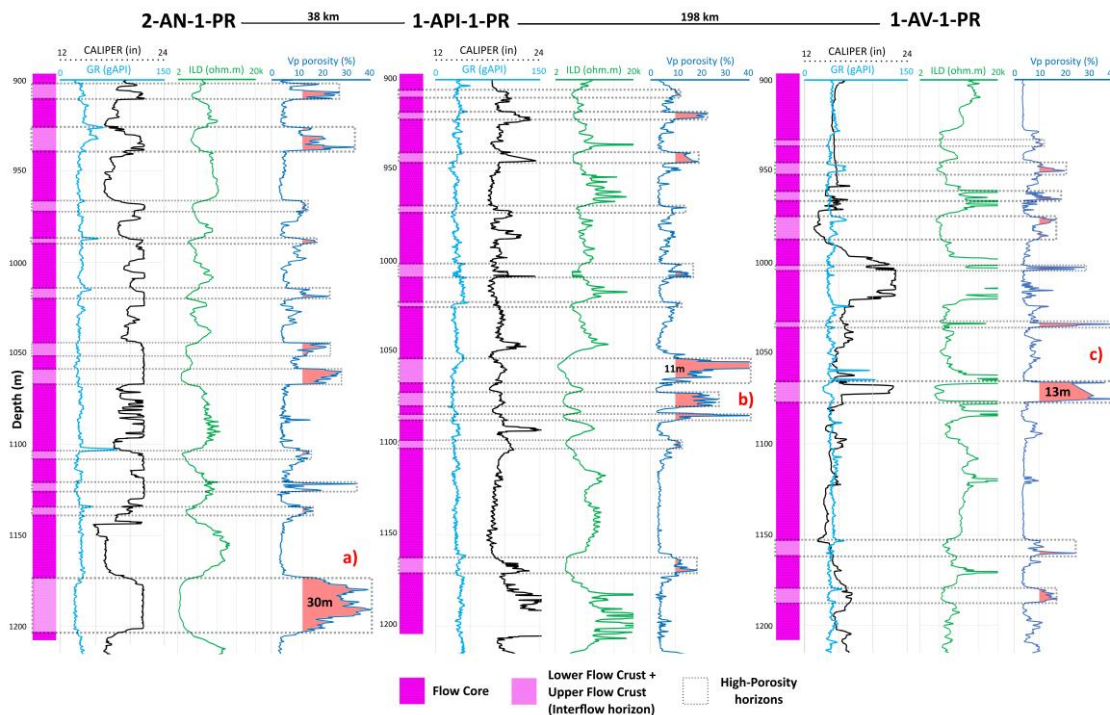


Figure 3. Analysed wells with the interpretation of high porosity horizons according to the geophysical data; a) 30-m high porosity interval; b) concentration of three high porosity intervals; c) clustering of three high-porosity intervals. Source: elaborated by the authors with data from ANP (2020).

Similarly, in well 1-AV-1-PR 11 high-porosity intervals were also identified (only 9 of them were delineated in the Figure 3 due to the resolution), with an average porosity of 17 %. Thicknesses vary from 0.8 to 12 m, averaging 2.2 m and summing to a total of 62 m. This yields a “net-to-gross” of 21%. A notable clustering of three high-porosity intervals within the 1,000 – 1,076 m (Figure 3c) depth range suggests a locally enhanced reservoir quality in well 1-AV-1-PR. The estimated temperature from the geothermal gradient for the 900 – 1,200 m interval ranges from 45 to 53°C. This depth interval aligns closely with similar high-porosity occurrences in well 1-API-1-PR, indicating a potential lateral correlation and continuity of favorable reservoir conditions across the area.

At flow boundaries (Interflow horizons) for all four wells, positive spikes in gamma ray values

4. FINAL REMARKS

The recurrence of high-porosity sections in these wells suggests that a geophysical interpretation can enhance the knowledge and help better plan a future injection well in

are observed, likely reflecting the presence of alteration minerals such as smectite and celadonite, as well as weathered zones (Planke, 1994; Nelson et al., 2015). Positive excursions in the caliper log further suggest the friable nature of the material, indicating collapse of the borehole walls in these high-porosity zones. In well 2-AN-1-PR, however, the caliper log behavior between 1,050–1,070 m and 1,175–1,200 m may indicate borehole breakouts, potentially leading to overestimated caliper readings and "net-to-gross" calculations.

Additionally, reduced ILD readings—reflecting increased electrical conductivity (the inverse of resistivity)—may indicate interconnected, fluid-filled porosity and/or elevated clay content (Planke, 1994; Nelson et al., 2015).

the SGG. Nonetheless, a pattern was observed, indicating a highly probable lateral continuity of the reservoir zones, enhancing the feasibility of CO₂ injection. The integrated workflow developed in this study improves our

understanding of the distribution of lava flows in the SGG and provides a robust initial framework for delineating intervals suitable for CO₂ injection. Future work will focus on spatially correlating these intervals at a sub-regional scale to further support CO₂ mineralization project planning and implementation in a specific location.

5. REFERENCES

ANDERSEN, M. S. et al. Log responses in basalt successions in 8 wells from the Faroe-Shetland channel – A classification scheme for interpretation of geophysical logs and case studies. Geological Society, London, Special Publications, v. 314, p. 364–391, 2009. Disponível em: <https://doi.org/10.1144/SP314.21> . Acesso em: 21 maio 2025.

ANP – AGÊNCIA NACIONAL DO PETRÓLEO, GÁS NATURAL E BIOCOMBUSTÍVEIS. REATE – Programa de Revitalização das Atividades de Exploração e Produção de Petróleo e Gás Natural em Áreas Terrestres. 2020. Disponível em: <https://reate.cprm.gov.br/anp/TERRESTRE> . Acesso em: 28 abr. 2025.

BROGLIA, C.; ELLIS, D. Effect of alteration, formation absorption, and standoff on the response of the thermal neutron porosity log in gabbros and basalts: Examples from Deep Sea Drilling Project-Ocean Drilling Program Sites. Journal of Geophysical Research: Solid Earth, v. 95, n. B6, p. 9171–9188, 1990. Disponível em: <https://doi.org/10.1029/JB095iB06p09171> . Acesso em: 21 maio 2025.

GISLASON, S. R. et al. Mineral sequestration of carbon dioxide in basalt: A pre-injection overview of the CarbFix project. International Journal of Greenhouse Gas Control, v. 4, n. 3, p. 537–545, 2010. Disponível em: <https://doi.org/10.1016/j.ijggc.2009.11.013> . Acesso em: 13 maio 2025.

HELM-CLARK, C. M.; RODGERS, D. W.; SMITH, R. P. Borehole geophysical techniques to define stratigraphy, alteration and aquifers in basalt. Journal of Applied Geophysics, v. 55, n. 1–2, p. 3–38, 2004. Disponível em: <https://doi.org/10.1016/j.jappgeo.2003.06.001> . Acesso em: 21 maio 2025.

Acknowledgments

The authors would like to thank Repsol Sinopec Brasil for supporting this research under the “DAC.SI Project” agreement, in accordance with the regulations of the National Agency of Petroleum, Natural Gas, and Biofuels (ANP) RD&I levy fund.

NAVARRO, J. et al. Assessing hydrofacies and hydraulic properties of basaltic aquifers derived from geophysical logging. Brazilian Journal of Geology, v. 50, n. 4, 2020. Disponível em: <https://doi.org/10.1590/2317-48892020200013> . Acesso em: 21 maio 2025.

NELSON, C. E. et al. Eocene volcanism in offshore southern Baffin Bay. Marine and Petroleum Geology, v. 67, p. 678–691, 2015. Disponível em: <https://doi.org/10.1016/j.marpetgeo.2015.06.010> . Acesso em: 13 maio 2025.

NELSON, C. E.; JERRAM, D. A.; HOBBS, R. W. Flood basalt facies from borehole data: implications for prospectivity and volcanology in volcanic rifted margins. Petroleum Geoscience, v. 15, n. 4, p. 313–324, 2009. Disponível em: <https://doi.org/10.1144/1354-079309-835> . Acesso em: 16 maio 2025.

OELKERS, E. H.; COLE, D. R. Carbon dioxide sequestration: A solution to a global problem. Elements, v. 4, n. 5, p. 305–310, 2008. Disponível em: <https://doi.org/10.2113/gselements.4.5.305> . Acesso em: 15 maio 2025.

OELKERS, E. H.; GISLASON, S. R.; MATTER, J. Mineral carbonation of CO₂. Elements, v. 4, p. 331–335, 2008. Disponível em: <https://doi.org/10.2113/gselements.4.5.333> . Acesso em: 9 maio 2025.

PLANKE, S. Geophysical response of flood basalts from analysis of wireline logs: Ocean Drilling Program Site 642, Vøring volcanic margin. Journal of Geophysical Research: Solid Earth, v. 99, n. B5, p. 9279–9295, 1994. Disponível em: <https://doi.org/10.1029/94JB00496> . Acesso em: 7 maio 2025.

RASOOL, M. H.; AHMAD, M.; AYOUB, M. Selecting geological formations for CO₂ storage: A comparative rating system. Sustainability, v. 15, n. 8, 6599, 2023. Disponível em: <https://doi.org/10.3390/su15086599> . Acesso em: 21 maio 2025.

ROSSETTI, L. M. et al. Evaluating petrophysical properties of volcano-sedimentary sequences: A case study in the Paraná-Etendeka Large Igneous Province. *Marine and Petroleum Geology*, v. 102, p. 638–656, 2019. Disponível em: <https://doi.org/10.1016/j.marpetgeo.2018.12.041> . Acesso em: 7 maio 2025.

SGB – SERVIÇO GEOLÓGICO DO BRASIL. Mapa geológico da bacia do Paraná. Porto Alegre: CPRM, 2022. Escala 1:1.000.000. Disponível em: <https://rigeo.cprm.gov.br/handle/doc/23037> . Acesso em: 10 maio 2025.

SHAW, J.; BACHU, S. Screening, evaluation, and ranking of oil reservoirs suitable for CO₂-flood EOR and carbon dioxide sequestration. *Journal of Canadian Petroleum Technology*, v. 41, n. 09, 2002. Disponível em: <https://doi.org/10.2118/02-09-05> . Acesso em: 22 abr. 2025.

ZIELINSKI, J. P. et al. Integrated GIS-modelling evaluation study of potential areas for the implementation of DACCS projects in the basalt formations of the Paraná Basin, Southern Brazil. In: 17th Greenhouse Gas Control Technologies Conference (GHGT-17), 20–24 out. 2024. 2024a. Disponível em: <https://dx.doi.org/10.2139/ssrn.5054696> . Acesso em: 14 maio 2025.

ZIELINSKI, J. P. et al. Initial insights into the geochemical reactivity of volcanic rocks from the Serra Geral Group (Paraná Basin, Brazil): a laboratory-scale perspective on in-situ mineralization. In: 17th Greenhouse Gas Control Technologies Conference (GHGT-17), 20–24 out. 2024. 2024b. Disponível em: <https://doi.org/10.2139/ssrn.5059245> . Acesso em: 14 maio 2025.